REPORT NO. DOT-TSC-FAA-72-5

PATH CHANGING METHODS APPLIED TO THE 4-D GUIDANCE OF STOL AIRCRAFT

ROBERT J. HYNES, LLOYD E. STEVENSON
TRANSPORTATION SYSTEMS CENTER
55 BROADWAY
CAMBRIDGE, MA. 02142

EDWARD B. CAPEN
SERVICE TECHNOLOGY CORPORATION
CAMBRIDGE, MA. 02142

transpo 72
U.S. International Transportation Exposition
Dulles International Airport
Washington, D.C.
May 27-June 4, 1972

NOVEMBER 1971
TECHNICAL REPORT

Prepared for:

DEPARTMENT OF TRANSPORTATION
FEDERAL AVIATION ADMINISTRATION
WASHINGTON, D.C. 20591

1. Report No.	2. Government Accession No.	3. Recipient's Catalog No.
DOT-TSC-FAA-72-5		

4. Title and Subtitle	5. Report Date
PATH CHANGING METHODS APPLIED TO THE 4-D GUIDANCE OF STOL AIRCRAFT	November 1971
	6. Performing Organization Code
7. Author(s) Robert J. Hynes, Edward B. Capen* and Lloyd E. Stevenson	8. Performing Organization Report No.
9. Performing Organization Name and Address Transportation Systems Center 55 Broadway Cambridge, MA 02142	10. Work Unit No. R2808
	11. Contract or Grant No. FA-218
12. Sponsoring Agency Name and Address Department of Transportation Federal Aviation Administration Washington, D.C. 20591	13. Type of Report and Period Covered Technical Report
	14. Sponsoring Agency Code

15. Supplementary Notes

*Service Technology Corporation
Cambridge, MA 02142

16. Abstract

Prior to the advent of large-scale commercial STOL service, some challenging navigation and guidance problems must be solved. Proposed terminal area operations may require that these aircraft be capable of accurately flying complex flight paths, and in some situations, maintaining a time of arrival envelope at waypoints along these paths (4-D guidance capability). This report discusses problems that arise in performing 4-D guidance and presents the results of an initial investigation of two candidate 4-D guidance schemes that are based on the aircraft having a limited amount of protected airspace for maneuvering. Preliminary analysis and simulation results are presented and future work on the 4-D guidance of STOLS is outlined. The results although presented for STOLS are applicable also to the 4-D guidance of any RNAV equipped aircraft.

17. Key Words	18. Distribution Statement
4-D Guidance, Flight Path Planning, Steering Laws	Availability is Unlimited. Document may be Released To the National Technical Information Service, Springfield, Virginia 22151, for Sale to the Public.

19. Security Classif. (of this report)	20. Security Classif. (of this page)	21. No. of Pages	22. Price
Unclassified	Unclassified	42	

TABLE OF CONTENTS

LIST OF ILLUSTRATIONS

LIST OF ILLUSTRATIONS (CONT.)

INTRODUCTION

The objective of this report is to describe work being done at DOT/TSC to develop 4-D guidance algorithms for STOL aircraft. The work described herein is primarily concerned with evaluating basic concepts and the integration of this research into an actual aircraft/ATC situation is not attempted. For the purposes of this study, it is assumed that the aircraft is RNAV equipped and has a limited onboard digital computation capability. The basic mission that the aircraft must fly, which includes 4-D waypoints and protected airspace limits, is assumed to be generated by a ground based metering and sequencing program and uplinked to the airborne system. Separation criteria are also assumed to be taken into account by the ground ATC system when specifying this mission and the protected airspace limits.

A functional block diagram of the airborne system is shown in Figure 1. The dashed segment of this block diagram represents the autocoupled system that was simulated on the hybrid computer in lieu of displays and a pilot to generate preliminary performance data on the systems being studied. In order to alleviate any ambiguity in the meaning of terminology as used in this

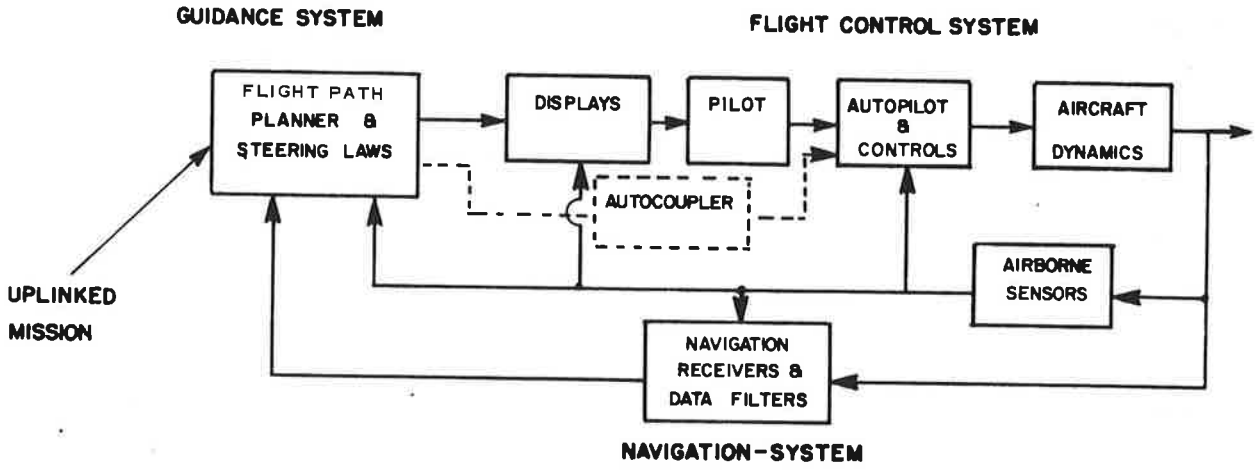

Figure 1. A Block Diagram of Airborne System

paper, the basic functions of the navigation system block and guidance system block are listed below:

> The Navigation System has the primary function of determining the position and if possible the velocity of the aircraft with respect to an earth-fixed coordinate system. This system is typically composed of radio wave receivers and the necessary computation capability to determine the state of the aircraft from the received information. For the simulation results contained herein perfect navigation and wind information was assumed.
>
> The Guidance System has the dual functions of generating the aircraft's flight path and also of generating the steering commands to keep the aircraft on this flight path. The flight path planner portion of the guidance system updates the guidance mission of the aircraft based upon the sensed aircraft state data, mission requirements and any predicted information that might be available. The steering law segment of the guidance system generates a velocity to be gained vector that is a function of the position and velocity error of the aircraft from a reference vehicle flying the mission prescribed by the flight path planner.

Two methods of doing 4-D guidance that are tailored to specific protected airspace situations are discussed. The flight path planners as currently implemented for both systems define constant airspeed missions taking into account winds such that the 4-D guidance requirements are satisfied within the allocated airspace. The main difference between the two planners is the method of moving the waypoints in order to do path stretching or compressing to lose or make up finite amounts of time.

The scenario for this research as previously stated considers a situation where the flight path planning is done onboard the aircraft. However, assuming accurate aircraft position and velocity information were available on the ground, the studied algorithms could be implemented on the ground and the 4-D guidance information uplinked to the aircraft. Also, as the protected airspace for maneuvering is reduced, both of these systems would become more dependent on speed adjustment to accomplish the 4-D guidance mission.

Performance Objectives

The philosoply that governed the performance goals of this work was to design a system that guided the aircraft as smoothly, as precisely and as efficiently as practicable while keeping the piloting workload and airborne computational requirements within reasonable limits. A method of satisfying the formentioned goals

would be to allow the aircraft to specify its own mission within the constraints of the ATC defined mission. This was done by assuming the aircraft could do limited extrapathway maneuvers from the nominal flight path to make up or lose finite amounts of time. If a limited maneuver capability is not present then the principle means of controlling time-of-arrival is through speed adjustment. This control channel is typically a slow response-time channel and the range of speed adjustment can be severely limited depending upon the operational situation of the aircraft. Speed control was therefore utilized as a secondary method of controlling time-of-arrival and was used only when the constraints on maneuvers did not allow the 4-D mission to be completed at constant airspeed.

STOL'S REQUIREMENT FOR A 4-D GUIDANCE CAPABILITY

Establishing the future need for a 4-D STOL guidance capability requires an understanding of the various urban-based markets that STOL may one day service and their implication on the air traffic patterns over the metropolitan area. An immediate and large volume market in which STOL may be found viable is in servicing the metropolises where the lack of airport capacity has caused air congestion. Of course, one ready answer to the lack of airport runways is to build more urban jet runways. But the requirement of new jet runways for large amounts of additional land has had the increasing effect of causing these new runways to be located outside the metropolitan areas they were designed to serve. STOL, with its relatively small land requirements and its relatively greater ability to fly around noise sensitive areas, could be the solution to the problem of establishing more urban runways. These runways would service the short-haul inter-city shuttle market to the relief of the existing jet runways. The intercity STOL shuttle would operate out of a system of stolports located either in the downtown area near the central business district, suburbia, or at the existing jetport or some combination of these. The final configuration will depend on local conditions such as community reaction and on market conditions such as the ability of STOL service to compete directly with existing CTOL service.

In operating into a STOL runway at a jetport, large scale STOL operations will be conducted in parallel with the CTOL operations. STOL operations will be independent of the CTOL traffic if their respective runways have sufficient distance between them. If not, the operations will be dependent and will be coordinated from the ground.

A second potential STOL market is in servicing the jetports that have been located outside of the metropolitan areas that they are to serve. The regional jetport STOL shuttle would operate out of a number of distributed small stolports within the metropolis and some sort of facility at the remote jetport. A third potential market available to STOL is the intraurban shuttle. The inhabitants of the large metropolitan areas are finding an increasing need for a high speed mode of travel within the metropolis itself to counter the increasing sprawl and congestion of urban life. The fourth and final potential STOL market is the intrastate/regional shuttle. While the city dweller has found himself increasingly restricted in travel due to sprawl and congestion, the country dweller finds himself increasingly isolated due to the curtailment of transportation services. A STOL shuttle system would link the regional centers of business, commerce, government, and the rural community with themselves and with their metropolitan hub. If the potential

of each of these markets is realized by STOL, there will be a profusion of air traffic criss-crossing the airspace above each metropolis. The air congestion that STOL seeks to relieve by making more runways available to intercity air traffic may be more than accounted for by the amount of air traffic generated in servicing these markets. A mature system of STOL services may be possible only if the traffic over the metropolitan area is highly coordinated.

4-D guidance can provide this coordination by giving the ATC system a much greater degree of control of an aircraft's position with respect to time. There are three distinct operational situations in which 4-D guidance may be of benefit. In independent operations into a runway, a controller meters and spaces the incoming aircraft. This coordination task is most difficult at runways operating near or at saturation. In the case of dependent operations into a runway, the controller has the additional task of coordinating the coupled operations. This situation could occur if an intercity STOL shuttle operated out of a STOL runway located at a metropolitan jetport. Finally, in the case of a large number of simultaneous operations within a confined airspace, coordination could be necessary once again. Whether STOL proves to be viable or not, the pressure of the continuing growth of CTOL traffic will one day require the coordination within the terminal area that 4-D guidance can provide. If STOL is successful in establishing large scale operations in these various urban-based markets, the need for and demands on coordination in the metropolitan terminal areas will indeed be even greater.

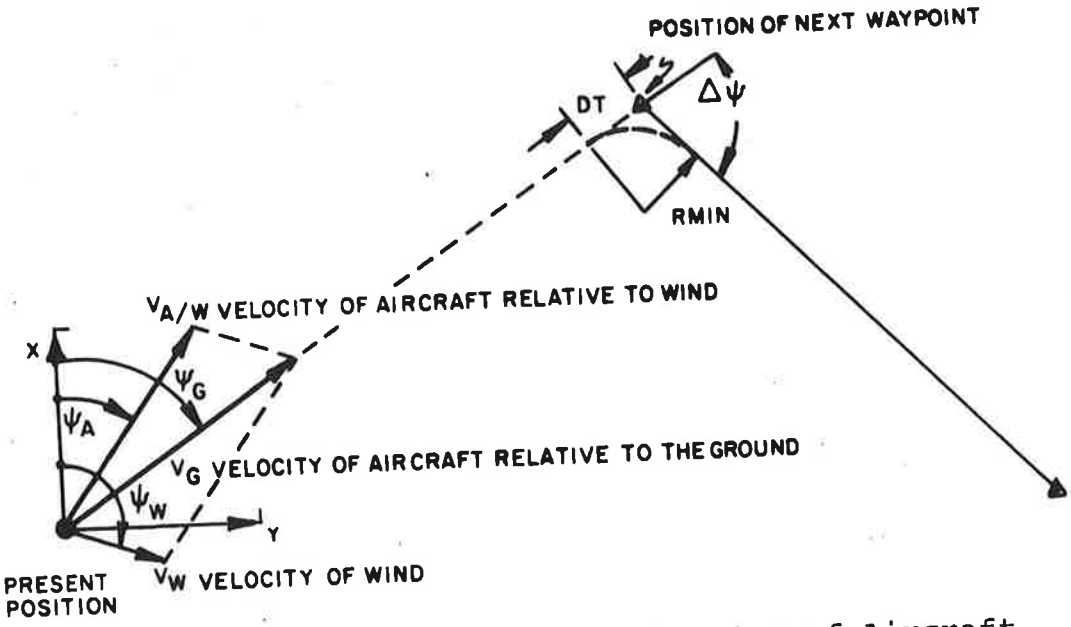

Figure 4 - Vector Diagram for Computation of Aircraft Velocity Relative to the Ground

the aircraft's present or initial condition in space and time can be computed utilizing the following recursive relationship:

$$t_f = t_i + \sum_{j=i}^{N-1} \frac{\Delta R_{j,j+1}}{V_{G_j}} + 2 \sum_{j=i}^{N-2} \frac{RMIN_{j,j+1}}{V_{G_j}} \left[\left| \frac{\Delta\psi_{j,j+1}}{2} \right| - \left(\frac{V_{G_j} + V_{G_{j+1}}}{2V_{G_{j+1}}} \right) \tan \left| \frac{\Delta\psi_{j,j+1}}{2} \right| \right] \quad (2)$$

This computed t_f is compared with the desired arrival time t_f^* and the waypoints are moved by the amount ΔM which is given by

$$\Delta M = AKM \ (t_f^* - t_f) \ VAF \quad (3)$$

where

AKM = iteration loop gain

t_f^* = ATC specified arrival time at the final waypoint

t_f = arrival time at the final waypoint for current computation cycle

VAF = weighted sum of the ground speed over the remainder of the mission

Figure 5 shows the variables used to define the direction of movement of the waypoints. This direction is defined as follows for the respective corners of the nominal mission:

$$\psi_{M_{pn}} = \psi_{pn-1} + \frac{\Delta\psi_{pn-1,\,pn}}{2} - \frac{\pi}{2}\,\text{sign}\,(\Delta\psi pn\text{-}1,\,pn) \qquad (4)$$

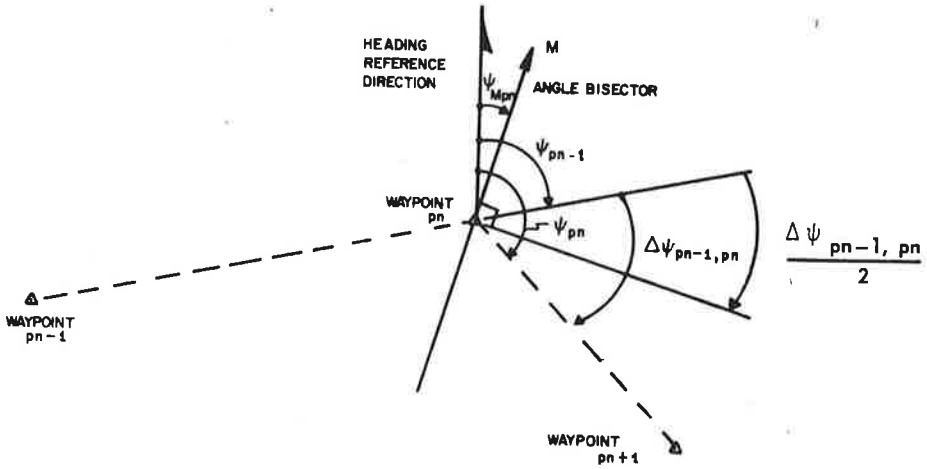

Figure 5. Waypoint Movement Variables and Geometry

Simulation Results for Corridor/Angle Bisector Guidance System

The corridor angle bisector guidance scheme was simulated on a Beckman 2200/XDS9300 hybrid computer. This simulation included the guidance system, a wind model and a Twin Otter aircraft/autopilot model as discussed in Appendix A.

The included results are based on the aircraft starting from waypoint 1 at an airspeed of 240 feet per second. Figures 6, 7, and 8 are computer generated plots of the aircraft's motion in the XY plane for nominal, early and late arrival times at waypoint 1 and for various wind conditions. From these figures the 100 seconds early situation is readily managed by this flight path planner. The 100 seconds late mission is seen to complete the first segment of the mission within the two nautical mile corridor but after the first turn the flight path

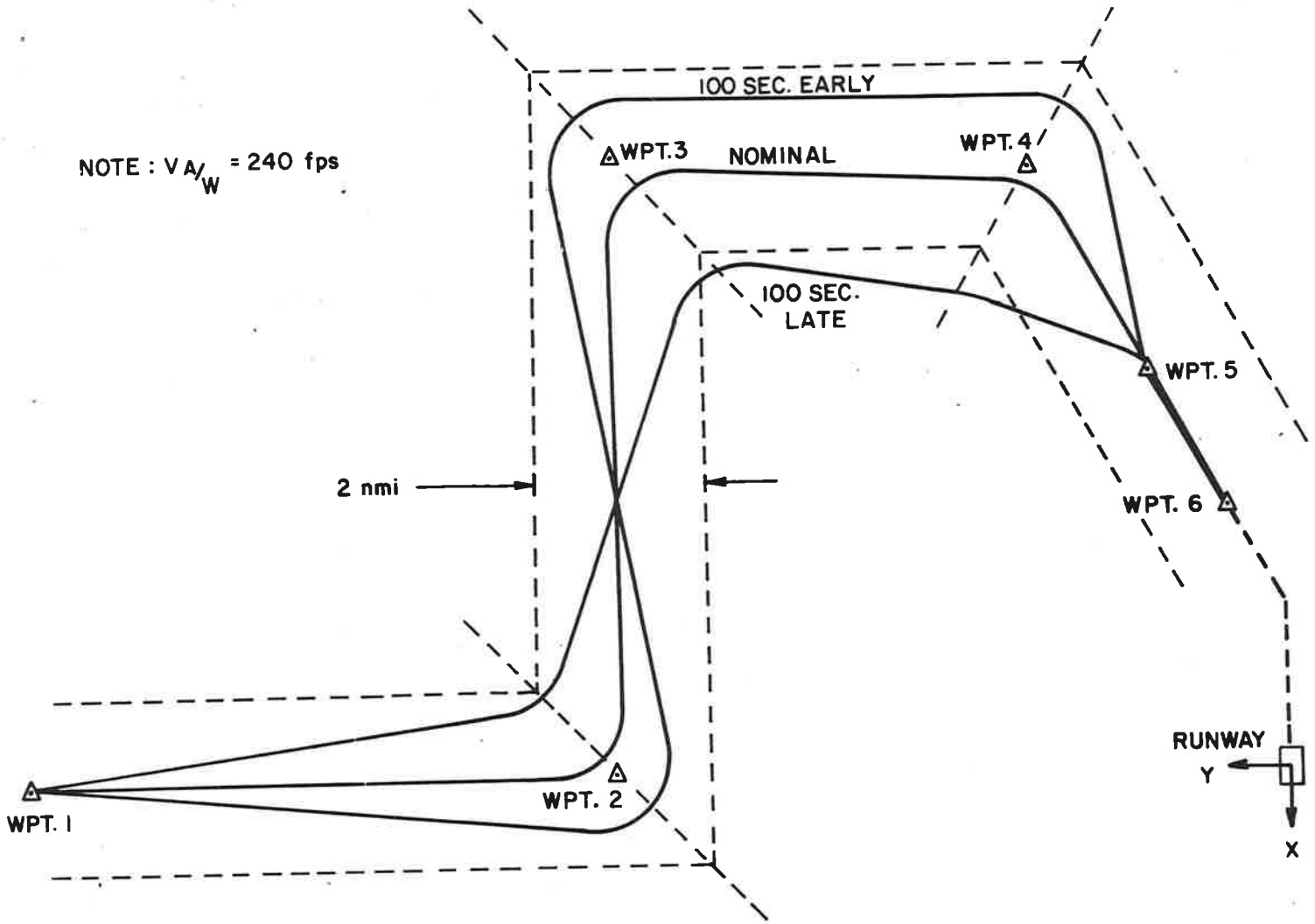

Figure 6. Flight Path Trajectories for Early, Late, and Nominal Arrival Time at Waypoint 1 (No Winds)

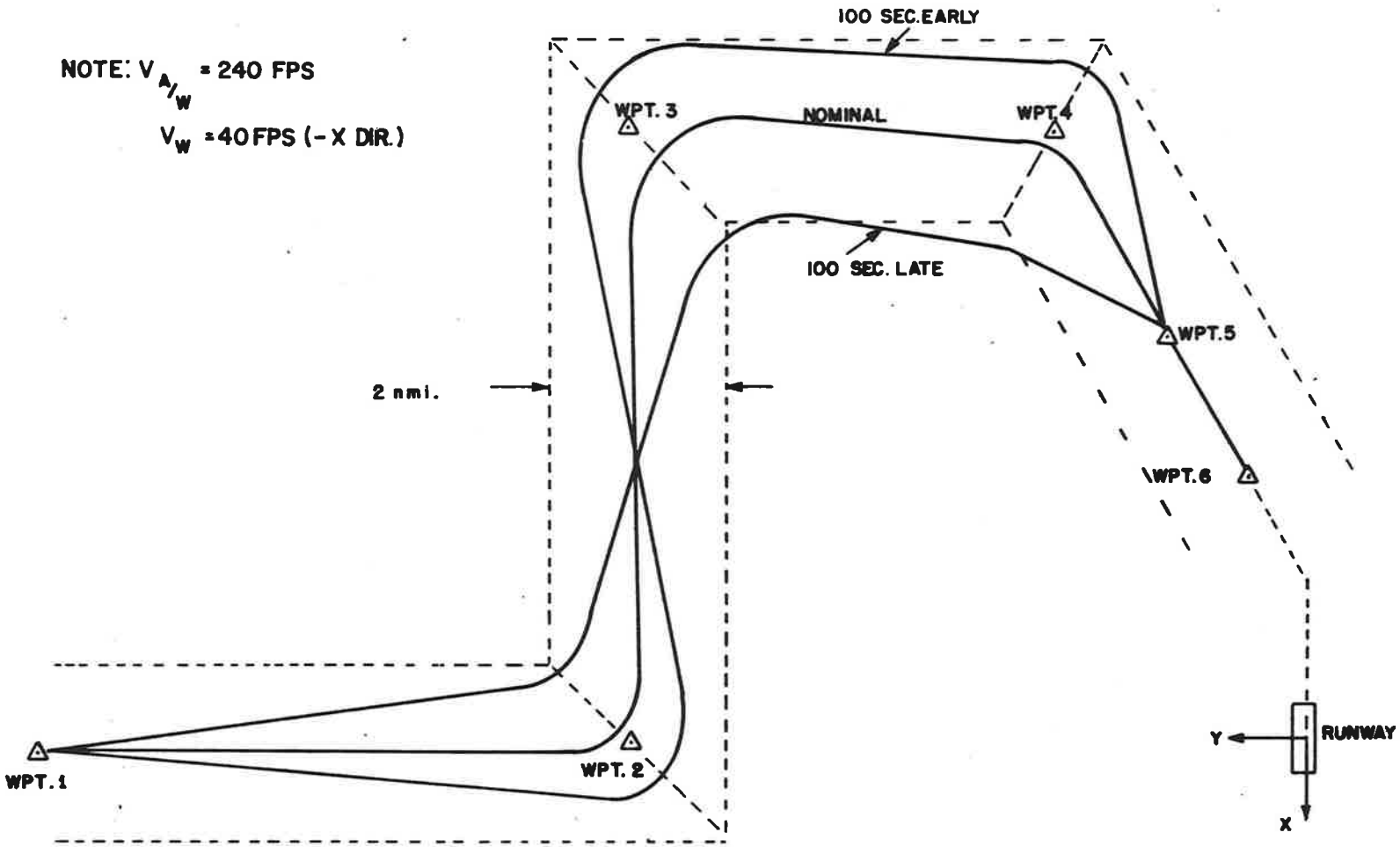

Figure 7. Flight Path Trajectories for Early, Late, and Nominal Arrival Time at Waypoint 1 (Steady Winds)

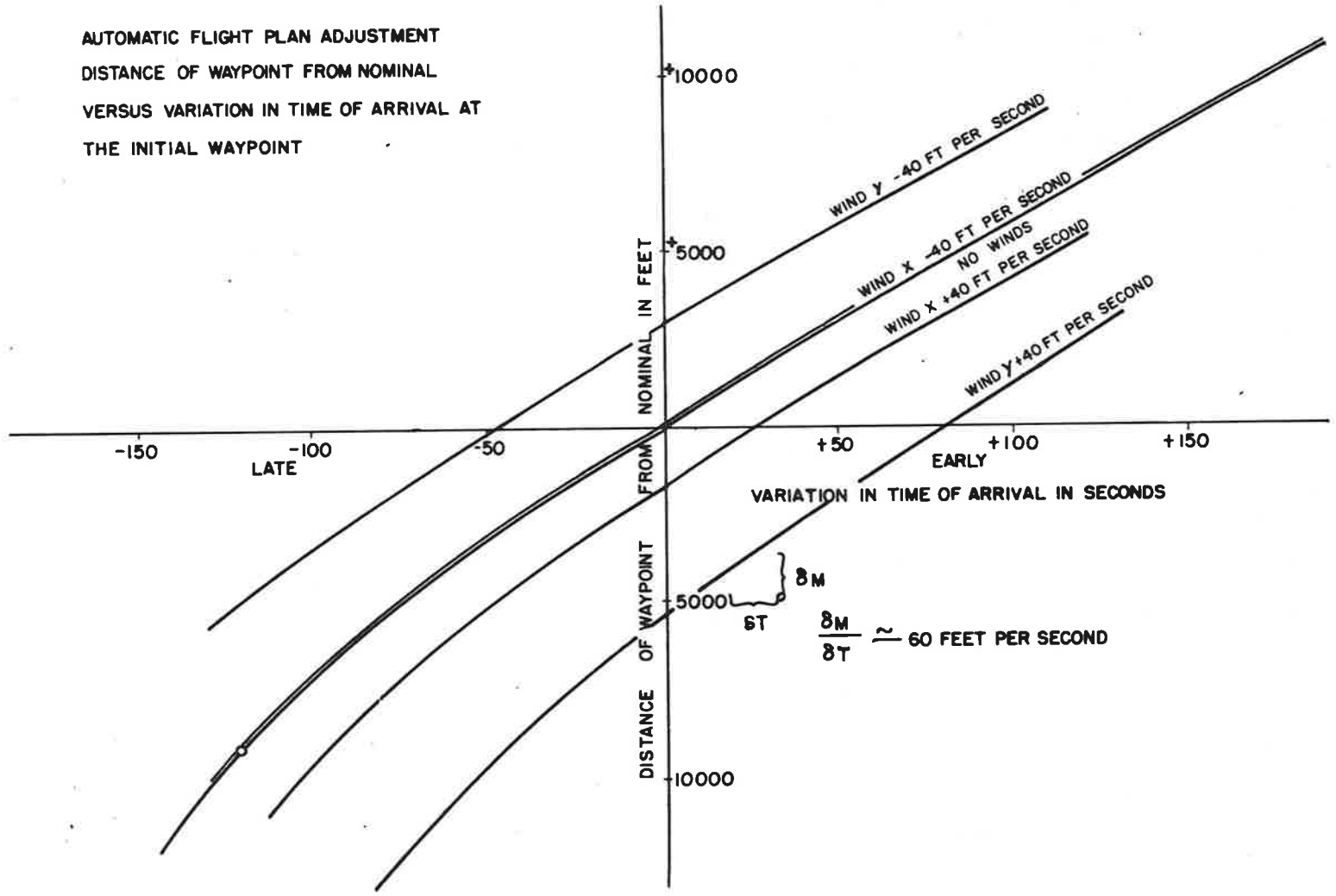

Figure 9. Waypoint Movement as a Function of Toa Error for Various Wind Conditions

DISCRETE MANEUVER VOLUME/TIME TO TURN FLIGHT PATH PLANNER

A protected airspace/path planner scheme that is currently under study but has not yet been integrated into the simulation is described in this section. The discrete maneuver volume/time to turn flight path planner utilizes the corners of the RNAV route to perform path stretching/compressing maneuvers. The time to turn flight path planner defines flight paths within these maneuver volumes that will rendezvous the aircraft with fixes located at the boundaries of the discrete maneuver volumes.

A possible terminal area RNAV route (STAR) with the discrete maneuver volumes at its corners is shown in Figure 10. The nominal mission is the same as defined in Figure 2 and the assumptions underlying the basic mission remain the same.

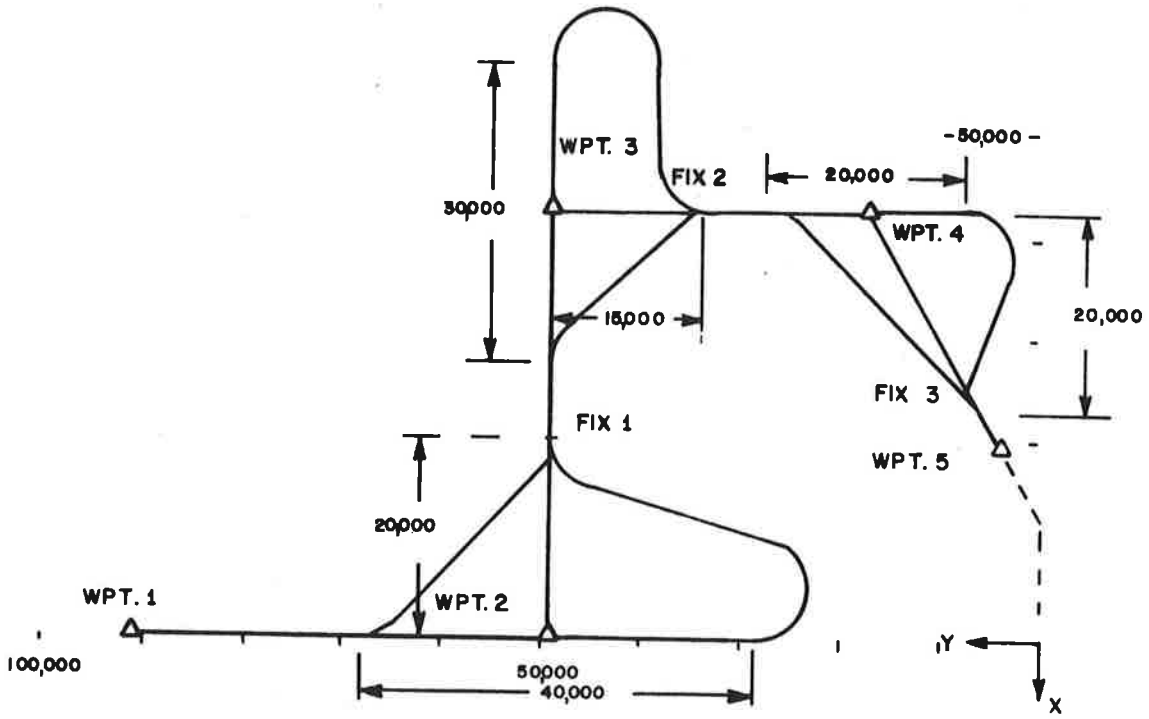

Figure 10. Discrete Maneuver Volume Protected Airspace

This flight planner is based upon choosing the proper point x1 to turn the aircraft such that it will rendezvous with a point x2 at a given time. Figure 11 shows three possible flight paths as defined by this flight path planner. The gain-time path starts the turn early and the lose time path delays the turn to stretch the trajectory. As can be readily seen, in

order for these flight paths to have any time of arrival control capability the nominal mission must have corners (6).

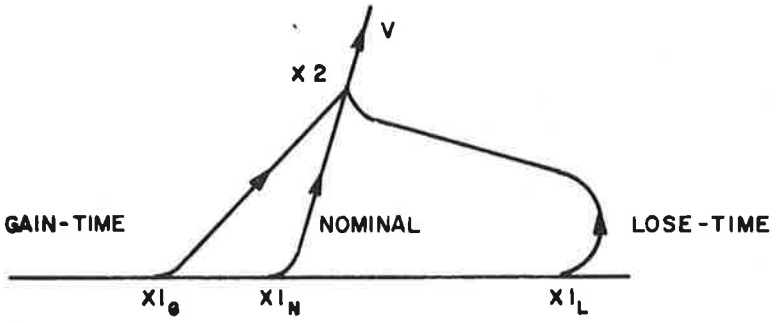

Figure 11. Possible Flight Paths as Defined by the Time to Turn Flight Path Planner

The time to turn subroutine involves computing the angles and lengths as shown in Figure 12 for the three situations that can arise. For a constant ground speed situation, the flight

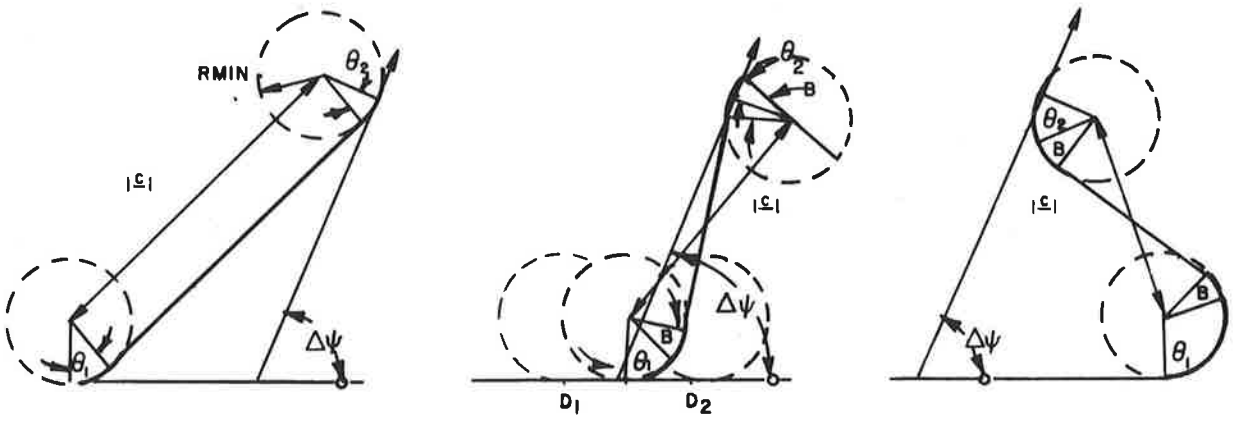

Figure 12. Three Situations for Time to Turn Computation

path length from the point xl to the point x2 for these three situations is as follows:

$$\text{(a)} \quad L_{12} = \text{RMIN}(|\theta_1|+|\theta_2|) + |\underline{c}| \tag{5}$$

$$\text{(b)} \quad L_{12} = \text{RMIN}(|\theta_1|-|\theta_2|+2|B|) + |\underline{c}| \cos B \tag{6}$$

$$\text{(c)} \quad L_{12} = \text{RMIN}(|\theta_1|+|\theta_2|+2|B|) + |\underline{c}| \cos B \tag{7}$$

where $|\underline{c}|$ is the center to center distance between the two circles of radius RMIN and RMIN is given by

$$RMIN = \frac{V^2}{g \cdot \tan|20°|} \tag{8}$$

The trajectories defined by this subroutine will be the minimum-time and minimum-maneuver flight paths to rendezvous with the point x2 with the constant velocity V for all xl if the point x2 lies at least a distance DMIN from the initial direction of travel (see Figure 13). DMIN is defined as follows:

$$DMIN = 3\ RMIN + RMIN \cos \Delta\psi \tag{9}$$

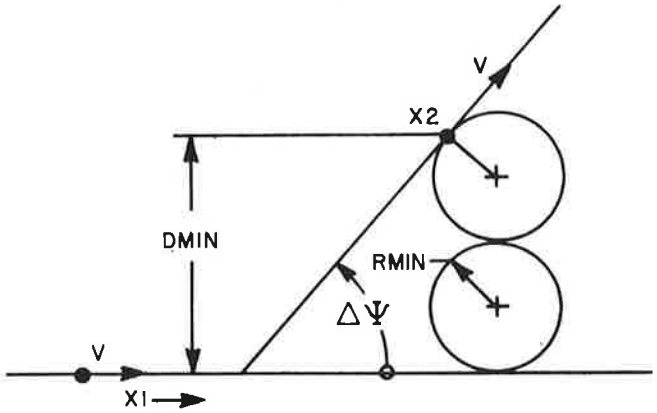

Figure 13. Minimum Separation Distance

Proposed Implementation Method

It is proposed that this flight path planner be implemented in the following manner. The flight planner will be called at the initiation of the mission to determine if the aircraft's speed needs to be changed. If a speed change were necessary, it would be immediately commanded. Prior to entering each maneuver volume, the flight planner would again be called to determine the time to turn the aircraft so that it would rendezvous with the specified fixes. The flight planner would attempt to null as much as possible of the time error in the maneuver volume the aircraft was entering, and then null the remaining error in the next maneuver volume etc.

Analytical Results for Discrete Maneuver Volume/Time to Turn Flight Path Planner

The discrete maneuver volume mission and the time to turn flight path planner were analyzed independent of the guidance and control systems and the aircraft dynamics model. Based on the results to date, this scheme would find its primary usefulness in doing fine tuning on the time of arrival of aircraft

at fixes in high density airspace. As will be shown, this method of controlling time of arrival has a limited gain-time capability. Also depending upon the dimensions of the maneuver volume and the amount of time to be lost, the lose-time missions may involve large turns since the turn requirements can increase with the amount of path stretching required.

The time of arrival control capability of the two 90° turns and the 60° turn for the maneuver volumes under consideration has been computed and is plotted in Figures 14, 15, and 16 for a ground speed of 240 fps. Utilizing this type of path stretching/compressing logic to control time of arrival is seen to give continuous (albeit bounded) time of arrival control. The total gain-time capability over the nominal time equals 91.2 seconds while the lose-time capability over the nominal time is 265 seconds. With the addition of a holding pattern at waypoint 1, the lose-time capability for the total mission would become infinite. Based upon being able to make up the maximum time of arrival error resulting from leaving a standard holding pattern (2 minutes or 1 minute with a 60 seconds advance callout), this discrete maneuver volume mission is seen to have a capability that lies between the two possible extremes.

For a no wind situation the maximum gain-time and lose-time missions would be the boundaries of the maneuver volumes as shown in Figure 10. The gain-time flight path is relatively simple to fly while the lose-time flight path involves large turns that could present difficult navigation problems. Results for a complete simulation of this system including aircraft/autopilot dynamics will be reported at a later date.

$$RMIN = \frac{V^2}{g \cdot \tan|20°|} \tag{8}$$

The trajectories defined by this subroutine will be the minimum-time and minimum-maneuver flight paths to rendezvous with the point x2 with the constant velocity V for all xl if the point x2 lies at least a distance DMIN from the initial direction of travel (see Figure 13). DMIN is defined as follows:

$$DMIN = 3\ RMIN + RMIN \cos \Delta\psi \tag{9}$$

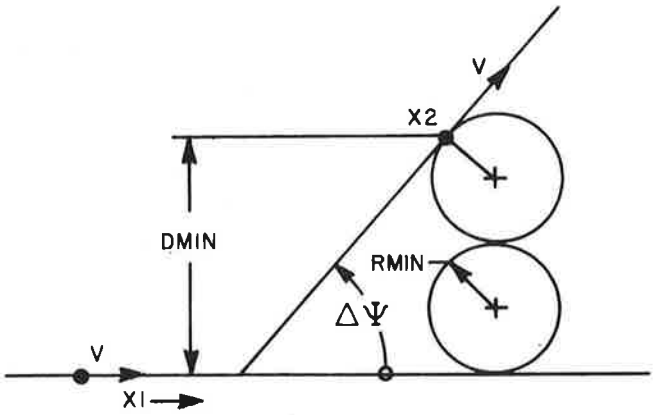

Figure 13. Minimum Separation Distance

Proposed Implementation Method

It is proposed that this flight path planner be implemented in the following manner. The flight planner will be called at the initiation of the mission to determine if the aircraft's speed needs to be changed. If a speed change were necessary, it would be immediately commanded. Prior to entering each maneuver volume, the flight planner would again be called to determine the time to turn the aircraft so that it would rendezvous with the specified fixes. The flight planner would attempt to null as much as possible of the time error in the maneuver volume the aircraft was entering, and then null the remaining error in the next maneuver volume etc.

Analytical Results for Discrete Maneuver Volume/Time to Turn Flight Path Planner

The discrete maneuver volume mission and the time to turn flight path planner were analyzed independent of the guidance and control systems and the aircraft dynamics model. Based on the results to date, this scheme would find its primary usefulness in doing fine tuning on the time of arrival of aircraft

at fixes in high density airspace. As will be shown, this method of controlling time of arrival has a limited gain-time capability. Also depending upon the dimensions of the maneuver volume and the amount of time to be lost, the lose-time missions may involve large turns since the turn requirements can increase with the amount of path stretching required.

The time of arrival control capability of the two 90° turns and the 60° turn for the maneuver volumes under consideration has been computed and is plotted in Figures 14, 15, and 16 for a ground speed of 240 fps. Utilizing this type of path stretching/compressing logic to control time of arrival is seen to give continuous (albeit bounded) time of arrival control. The total gain-time capability over the nominal time equals 91.2 seconds while the lose-time capability over the nominal time is 265 seconds. With the addition of a holding pattern at waypoint 1, the lose-time capability for the total mission would become infinite. Based upon being able to make up the maximum time of arrival error resulting from leaving a standard holding pattern (2 minutes or 1 minute with a 60 seconds advance callout), this discrete maneuver volume mission is seen to have a capability that lies between the two possible extremes.

For a no wind situation the maximum gain-time and lose-time missions would be the boundaries of the maneuver volumes as shown in Figure 10. The gain-time flight path is relatively simple to fly while the lose-time flight path involves large turns that could present difficult navigation problems. Results for a complete simulation of this system including aircraft/autopilot dynamics will be reported at a later date.

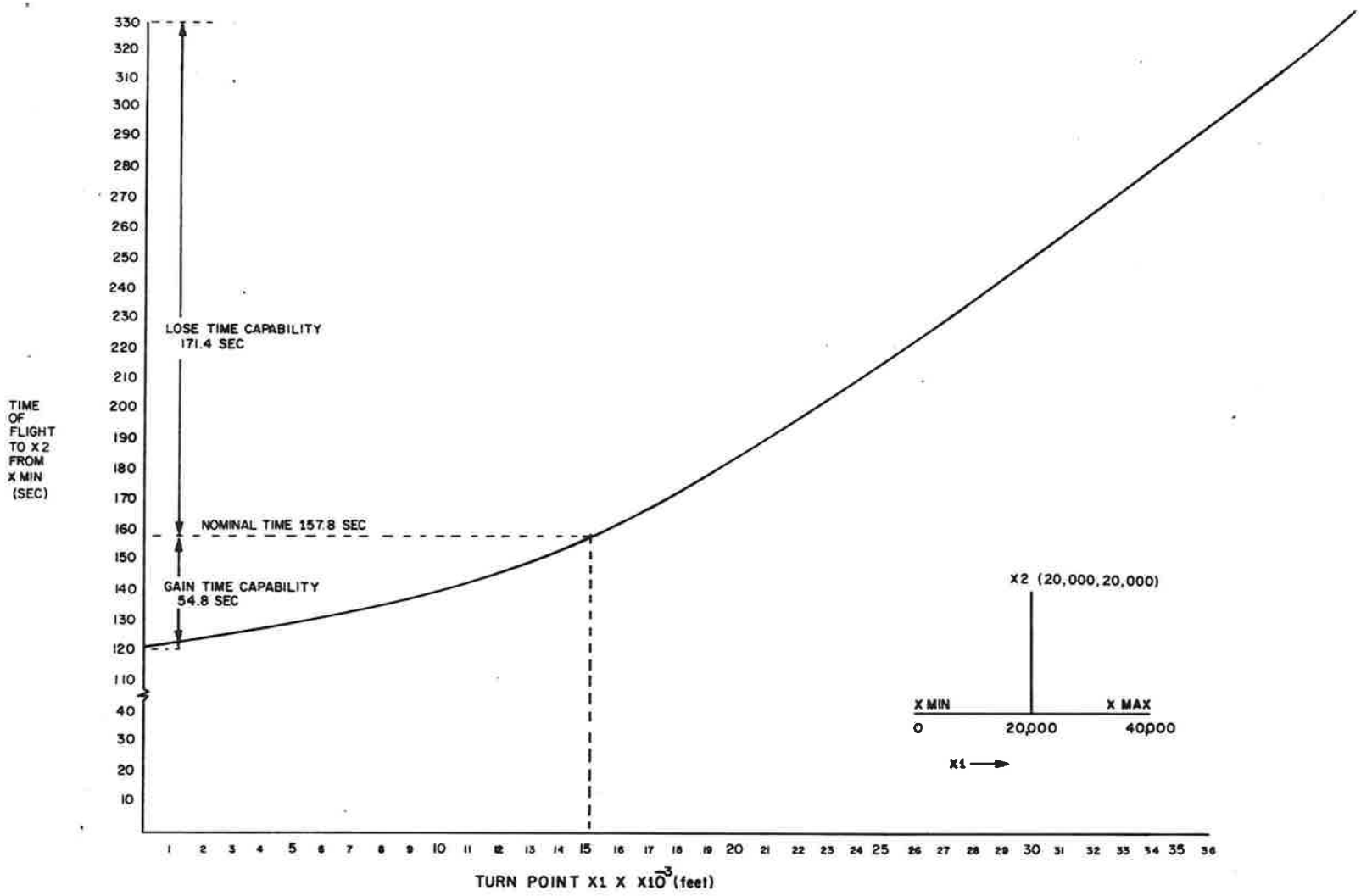

Figure 14. Flight Time from XMIN to X2 for Various Turn Points X1 for Discrete Maneuver Volume 1

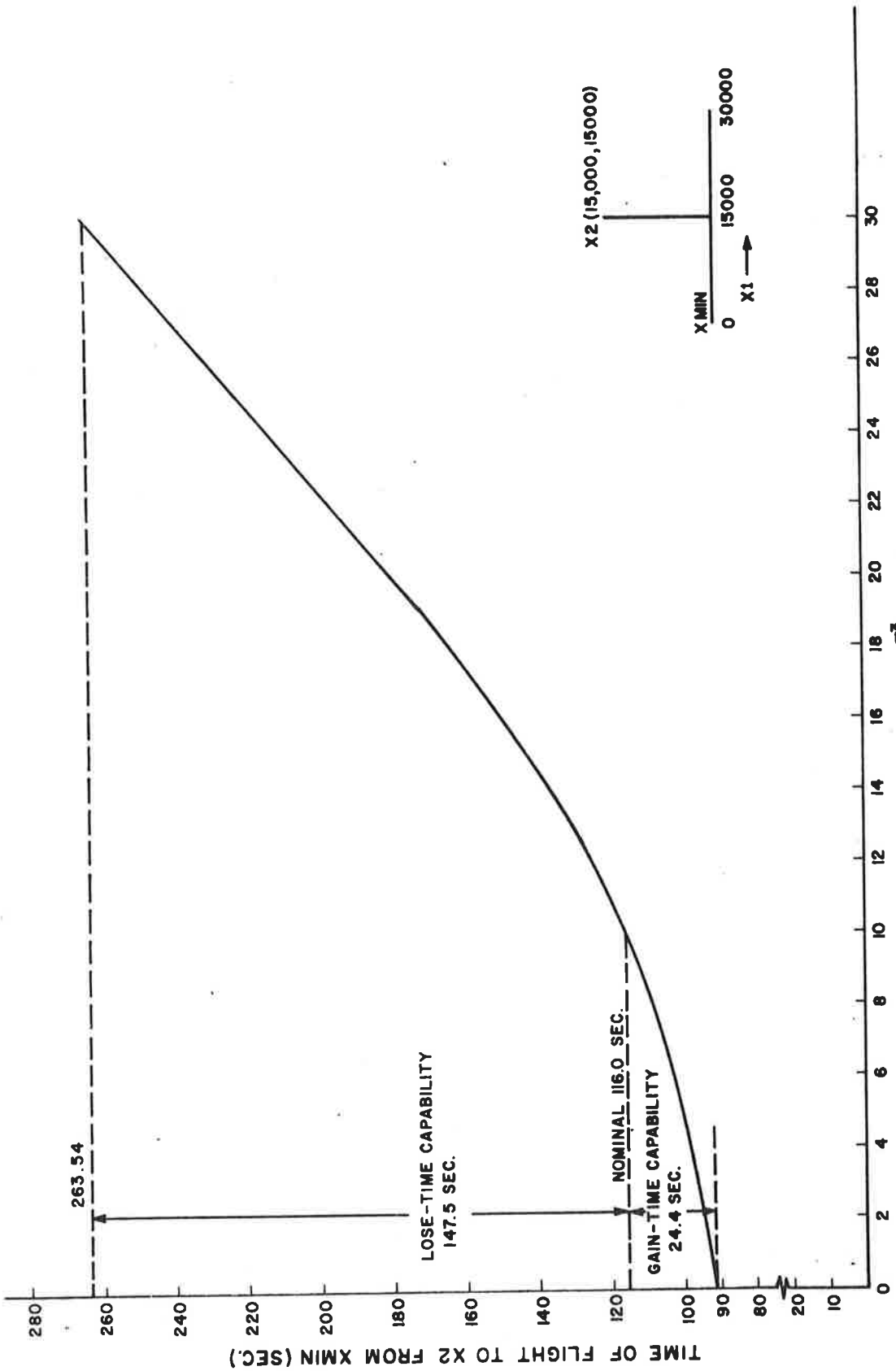

Figure 15. Flight Time from XMIN to X2 for Various Turnpoints X1 for Discrete Maneuver Volume 2

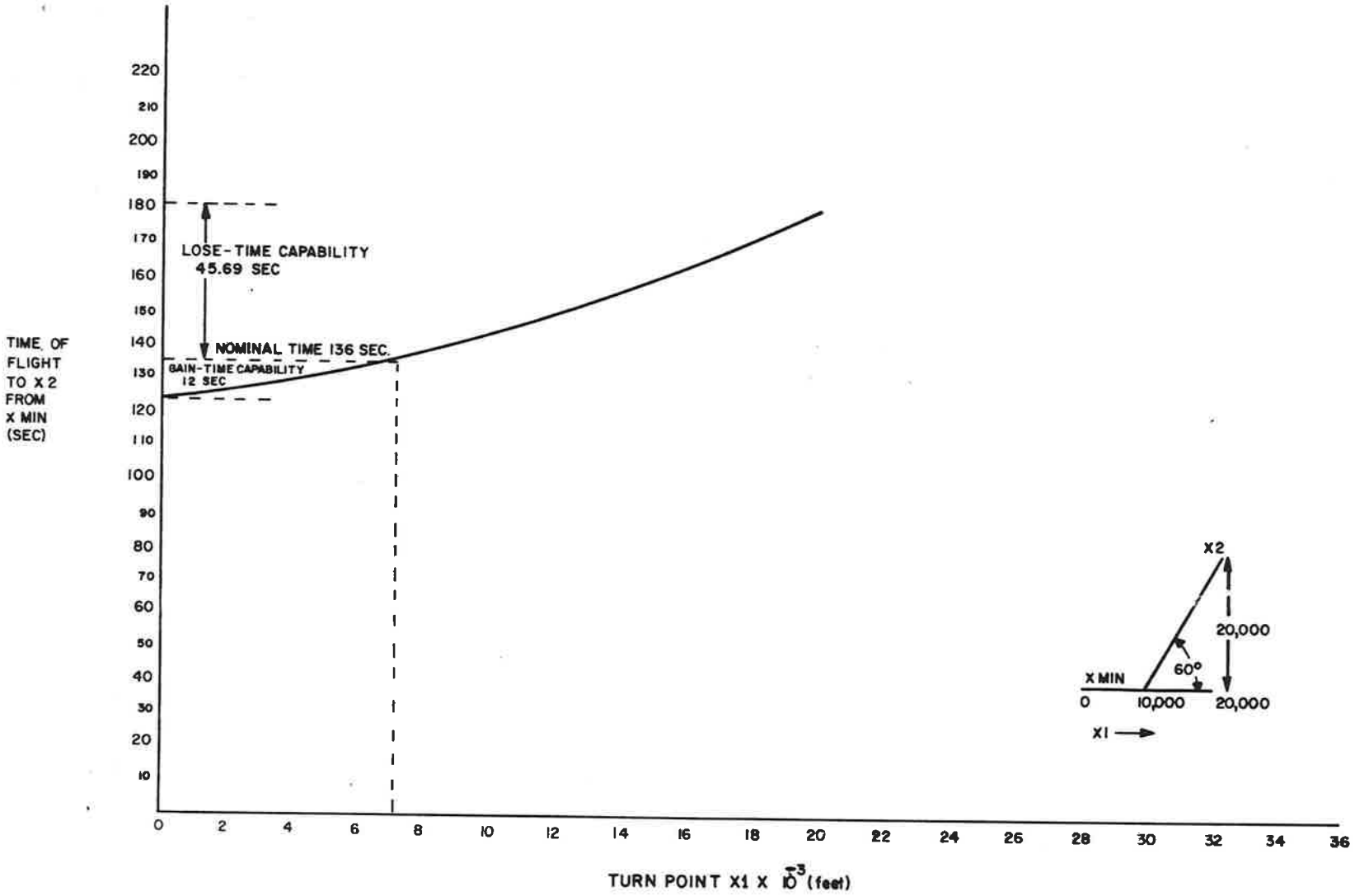

Figure 16. Flight Time from XMIN to X2 for Various Turnpoints X1 for Discrete Maneuver Volume 3

CONCLUSIONS AND RECOMMENDATIONS FOR FUTURE WORK

This paper considers two methods of doing 4-D guidance for a given mission where the cockpit has the capability of defining its own mission within the constraints of the ATC defined mission. The preliminary computer results on the corridor/angle bisector guidance scheme demonstrate that it is possible to do precise 4-D guidance in the face of constant wind disturbances and aircraft/autopilot dynamics assuming perfect navigation and wind information. The corridor/angle bisector flight planner and the guidance and steering system as realized in this simulation required about 2K of 24 bit word computer memory. This does not represent a large memory requirement and it is felt that this requirement could be reduced to 1.5K for an actual implementation. The iteration loop convergence rate was excellent and a typical time for iterating a new mission was .01 seconds.

If this flight planner and guidance system could be implemented in an aircraft, it is felt that the following performance objectives could be realized:

1. The ATC operating efficiency could be increased and the ATC workload decreased by curtailling the amount of direct intervention by the ATC system in realizing 4-D guidnace.

2. The aircraft operating cost could be decreased due to the aircraft's ability to define a mission more commensurate with its operational capabilities and due to the increased efficiency of the ATC system.

3. The pilot workload could be decreased due to the capability of the flight path planner to define a constant airspeed mission with a near minimum of heading changes (within the allowed airspace constraints).

4. The passenger comfort could be increased due to the capability of the flight path planner to define a smooth guidance mission with a near minimum of speed and heading changes (within the allowed airspace constraints).

It is difficult to compare the two candidate systems in detail since they were both tailored to a specific protected airspace situation and only the angle bisector scheme was actually simulated. The corridor angle bisector flight path planner defined missions that in general were easy to navigate

and fly, and in an overall sense these flight paths remained relatively close to the nominal flight path. Whereas when implemented, the discrete maneuver volume/time to turn flight path planner would force the aircraft to return as quickly as possible to the nominal mission and by restricting the maneuvers to the discrete portions of the airspace it would be much easier for the ATC system to determine the intent of user aircraft.

References

1. Bryson, A.E., Application of Optimal Control Theory in Aerospace Engineering, AIAA Journal of Spacecraft and Rockets, Vol. 4, No. 5, May 1967.

2. Connor, M.A., Optimization of Lateral Turns at Constant Height, AIAA Journal Vol. 5, No. 1, January 1967.

3. Bryson, A.E., and Lele, M.M., Minimum Fuel Lateral Turns at Constant Altitude, AIAA Journal Vol. 7, No. 3, March 1969.

4. Erzberger, H. and Lee, H.Q., Optimum Horizontal Guidance Techniques for Aircraft, AIAA Journal of Aircraft, Vol. 8, No. 2, Feb. 1971.

5. Miele, A., Flight Mechanics Vol. 1 Theory of Flight Paths, Addison-Wesley, Reading, Mass., 1962.

6. Holland, F.G. et al., Genealogy of Terminal ATC Automation, Mitre Corp. Report M70-9, Washington, D.C., February 1970.

7. MacDonald, R.A. et al., Linearized Mathematical Models for DeHavilland Canada "Buffalo & Twin Otter" STOL Transports Report No. DOT-TSC-FAA-71-8, June 1971.

APPENDIX A

AIRCRAFT/AUTOPILOT DESCRIPTION

A constant coefficient aircraft dynamics model along with a ϕ_c, θ_c, U_c autopilot were used to evaluate the various guidance schemes in a closed loop fashion. The longitudinal motion was represented by the following three dynamics equations:

$$\dot{U} = \frac{1}{m}\left[X_U\ (U - U_o) + X_W\ W + X_Y\ \delta_T\right] \tag{A1}$$

$$\dot{Q} = \frac{1}{I_{yy}}\left[M_Q Q + M_{\dot{W}}\dot{W} + M_W W + M_{\delta_E}\ \delta_E\right] \tag{A2}$$

$$\dot{W} = \frac{1}{m - Z_{\dot{W}}}\left[Z_W W + mUQ + Z_Q Q + Z_{\delta_E}\ \delta_E\right] \tag{A3}$$

For the lateral/directional motion it was assumed that all turns were coordinated and that the aircraft dynamics could adequately be described by the single moment equation.

$$P = \frac{1}{I_x}\left[L_P P + L_{\delta_A}\ \delta_A\right] \tag{A4}$$

The values of the dimensional stability derivatives were based on reference [7].

The ϕ_c and θ_c autopilot loops were designed for quick response and no overshoot ($\xi = .707$). The U_c autopilot subsystem was designed so that the dominant root was on the real axis with a time constant of two seconds. The autopilot block diagrams for the various channels are shown in Figure A-1.

The aircraft's motion was simulated with respect to a set of earth fixed coordinates with the X and Y axes lying in the horizontal plane and the Z axis of the orthogonal triad pointing into the earth. The X axis was also utilized as the bearing reference axis.

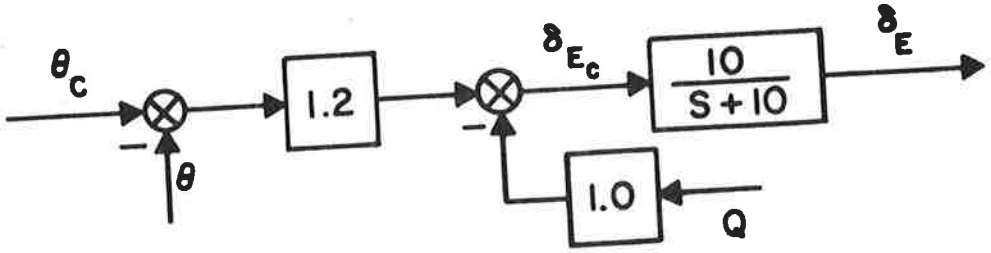

a) θ_c Loop

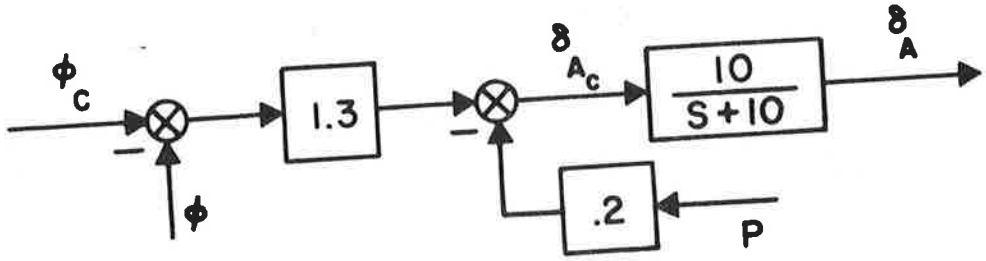

b) ϕ_c Loop

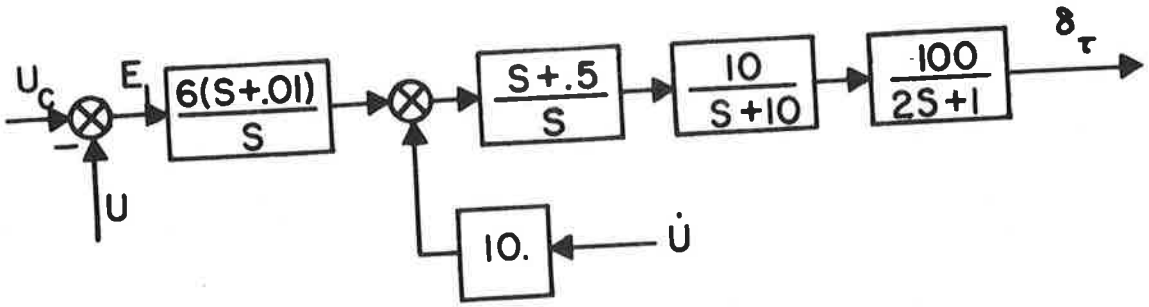

c) U_c Loop

Figure A1. Autopilot Block Diagrams

APPENDIX B

ANGLE BISECTOR FLIGHT PATH PLANNER DESCRIPTION AND EQUATIONS

This appendix contains a description and detailed equations for the angle bisector flight path planner. This flight path planner defines an updated 4-D guidance mission for the aircraft that takes into account the effects of the wind and the current position of the aircraft in space and time. As mentioned previously, it is assumed the ATC center uplinks the nominal 4-D waypoints X_{pn}, Y_{pn}, Z_{pn}, T_{pn} which are defined with respect to an earth-fixed reference system and a specified time base. Besides the waypoints the following information is also known or assumed known by the flight planner:

$\bar{V}_W$ = wind velocity vector.

$V_{A/W}$ = airspeed of aircraft.

$V_{A/W\ max}$, $V_{A/W\ min}$ = maximum and minimum allowable airspeeds, respectively.

X, Y, Z = components of the aircraft's position vector with respect to an earth-fixed reference system.

$\dot{X}$, $\dot{Y}$, $\dot{Z}$ = components of the aircraft's velocity vector with respect to an earth-fixed reference system.

The flight path planner subroutine contains the following three basic parts:

1. The computation of the velocity of the aircraft relative to the ground for each leg.
2. The time of arrival at the final waypoint computation.
3. The waypoint adjustment computation.

The program proceeds as follows:

I. Velocity of the Aircraft Relative to the Ground

From the present position to the next waypoint and between the remaining waypoints the following difference vector is computed (see Figure 4):

$$\begin{bmatrix} \Delta X_j \\ \Delta Y_j \end{bmatrix} = \begin{bmatrix} X_{j+1} - X_j \\ Y_{j+1} - Y_j \end{bmatrix} \tag{B1}$$

and these differences are used to compute

$$\Delta R_j = \sqrt{\Delta X_j^2 + \Delta Y_j^2}$$

In the following derivations the subscript j will be dropped for convenience although these computations must be done for each leg. The sine and cosine of the heading angle for each leg are given by

$$\sin \psi_G = \Delta Y/\Delta R \tag{B2}$$

$$\cos \psi_G = \Delta X/\Delta R \tag{B3}$$

thus,

$$\psi_G = \text{ARCTAN } (\sin \psi_G/\cos \psi_G) \tag{B4}$$

where $-\pi < \psi_G \leq \pi$. The difference angle between the aircraft's heading angle and the ground path heading is computed as follows from the law of sines:

$$\sin (\psi_A-\psi_G) = \frac{V_{WX}}{V_{A/W}} \sin \psi_G - \frac{V_{WY}}{V_{A/W}} \cos \psi_G \tag{B5}$$

and assuming the wind velocity will not exceed the airspeed of the aircraft

$$\cos (\psi_A-\psi_G) = \sqrt{1-\sin^2 (\psi_A-\psi_G)} \tag{B6}$$

$$\psi_A - \psi_G = \text{ARCTAN } \left(\sin (\psi_A-\psi_G) \Big/ \cos (\psi_A-\psi_G)\right) \tag{B7}$$

where $-\pi/2 < \psi_A - \psi_G < \pi/2$. The heading of the airspeed vector is then given by

$$\psi_A = (\psi_A-\psi_G) + \psi_G \tag{B8}$$

The ground speed required to compute the flight time for each leg is as follows:

$$\begin{bmatrix} V_{GX} \\ V_{GY} \end{bmatrix} = \begin{bmatrix} V_{WX} + V_{A/W} \cos \psi_A \\ V_{WY} + V_{A/W} \sin \psi_A \end{bmatrix} \tag{B9}$$

therefore, the ground speed is given by

$$V_G = \sqrt{V_{GX}^2 + V_{GY}^2} \tag{B10}$$

II. Time of Flight Computation

The time of flight to the final waypoint computation involves summing the flight times for the straight parts of the flight and the flight times in the turns. Figure B1 shows the pertinent terms used in this computation. A recursive relationship can be defined for the arrival time at the final point by considering the arrival times at the points t_2, t_3, t_4, and t_5. The arrival time at t_2 starting at the point t_1 is given by

$$t_2 = t_1 + \Delta T_{12} + \frac{RMIN_{12}}{V_{G1}} \left[2 \left| \frac{\Delta\psi_{12}}{2} \right| - \tan \left| \frac{\Delta\psi_{12}}{2} \right| \right]$$

and the time of arrival at the point t_3 from t_2 would be

$$t_3 = t_2 + \Delta T_{23} + \frac{RMIN_{23}}{V_{G2}} \left[2 \left| \frac{\Delta\psi_{23}}{2} \right| - \tan \left| \frac{\Delta\psi_{23}}{2} \right| \right] - \frac{RMIN_{12}}{V_{G2}} \tan \left| \frac{\Delta\psi_{12}}{2} \right|$$

Continuing in this manner, the arrival time at the final waypoint is given by

$$t_f = t_5 + \Delta T_{56} - \frac{RMIN_{45}}{V_{G5}} \tan \left| \frac{\Delta\psi_{45}}{2} \right|$$

Substituting the times t_4, t_3, t_2 into this equation gives the following recursive relationship for the t_f computation

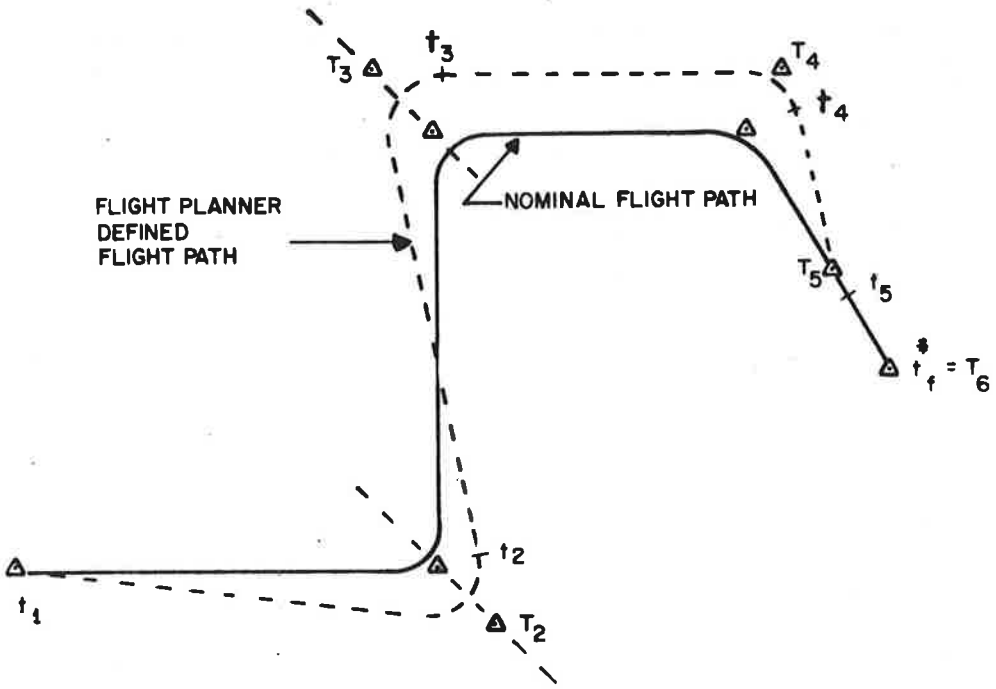

Figure B1. Time of Flight Computation Terminology

$$t_f = t_i + \sum_{j=i}^{N-1} \Delta T_{j,j+1} + \sum_{j=i}^{N-2} \frac{2RMIN_{j,j+1}}{V_{G_j}} \left[\left| \frac{\Delta\psi_{j,j+1}}{2} \right| - \left(\frac{V_{G_j} + V_{G_{j+1}}}{2V_{G_{j+1}}} \right) \tan \left| \frac{\Delta\psi_{j,j+1}}{2} \right| \right] \quad \text{(B11)}$$

where for the case of starting at point 1 the variable i would equal 1. Because Eq. (B11) involves a transcendal function, an iterative process was needed to define the revised mission.

III. Waypoint Adjustment Computation

In order to close the iteration loop, the waypoints are moved according to the error in the time of arrival as follows:

$$\Delta M = AKM \ (t_f^* - t_f) \ VAF \quad \text{(B12)}$$

where

$$AKM = .2$$

t_f^* = desired time of arrival at the final point

$$VAF = \sum_{j=i}^{N} \frac{(T_{j+1} - T_j)}{t_f^* - t_i} V_{G_j}$$

The adjusted waypoints then become

$$\begin{bmatrix} X_{pn} \\ Y_{pn} \end{bmatrix} = \begin{bmatrix} X_{pn} + \Delta M \cos \psi_{M_{pn}} \\ Y_{pn} + \Delta M \sin \psi_{N_{pn}} \end{bmatrix} \tag{B13}$$

where the X_{pn} and Y_{pn} on the right side are the components of the previous waypoint. The angle $\psi_{M_{pn}}$ is the bisector angle properly directed and is given by

$$\psi_{Mpn} = \psi_{pn-1} + \frac{\Delta\psi_{pn-1,pn}}{2} - \frac{\pi}{2} \text{ sign } (\Delta\psi_{pn-1,pn}) \tag{B14}$$

When the iteration loop has reduced the time of arrival error to within $\pm$.5 seconds, the 4-D waypoints as specified by the flight planner are input to the guidance and steering system.

APPENDIX C

STEERING LAWS

Regulation of the aircraft's position and velocity from start to finish is required to insure that the vehicle accomplishes its mission and remains within protected airspace. This regulation is accomplished by generating steering commands based on a reference vehicle which flies in position, velocity and acceleration the flight planner specified mission.

The 4-D waypoints as defined in the flight path planner provide the basic mission profile for the reference vehicle's motion. For the straight portions of the mission the reference vehicle's velocity and position as a function of time are given by:

$$\begin{bmatrix} \dot{X}_r \\ \dot{Y}_r \\ \dot{Z}_r \end{bmatrix}_S = \frac{1}{T_{pn+1} - T_{pn}} \begin{bmatrix} X_{pn+1} - X_{pn} \\ Y_{pn+1} - Y_{pn} \\ Z_{pn+1} - Z_{pn} \end{bmatrix} \tag{C1}$$

$$\begin{bmatrix} X_r \\ Y_r \\ Z_r \end{bmatrix}_S = \begin{bmatrix} X_{pn+1} - (T_{pn+1} - t)\,\dot{X}_r \\ Y_{pn+1} - (T_{pn+1} - t)\,\dot{Y}_r \\ Z_{pn+1} - (T_{pn+1} - t)\,\dot{Z}_r \end{bmatrix} \tag{C2}$$

where the pn subscripted quantities on the right hand sides of Eqs. (C1) and (C2) are based on the 4-D waypoints defined by the flight planner. The reference vehicle's velocity and position while in the turns are given by:

$$\begin{bmatrix} \dot{X}_r \\ \dot{Y}_r \\ \dot{Z}_r \end{bmatrix}_T = \begin{bmatrix} V \cos\,(\dot{\psi}t + \psi_o) \\ V \sin\,(\dot{\psi}t + \psi_o) \\ 0 \end{bmatrix} \tag{C3}$$

$$\begin{bmatrix} X_r \\ Y_r \\ Z_r \end{bmatrix}_T = \begin{bmatrix} X_o + \frac{V}{\dot{\psi}} \left(\sin\ (\psi_o+\dot{\psi}t) - \sin\ (\psi_o)\right) \\ Y_o - \frac{V}{\dot{\psi}} \left(\cos\ (\psi_o+\dot{\psi}t) - \cos\ (\psi_o)\right) \\ Z_r \end{bmatrix} \qquad \text{(C4)}$$

where

X_o = x component of position vector at turn initiation

Y_o = y component of position vector at turn initiation

ψ_o = heading of reference vehicle at turn initiation

$V = \sqrt{\dot{X}_r^2 + \dot{Y}_r^2}$ ($\dot{X}_r$ and $\dot{Y}_r$ are computed using Eqs. (C1) and are based on the leg preceding the turn)

$$\dot{\psi} = \frac{g \tan\ (20°)}{V} \text{ sign } (\Delta\psi)$$

The time to start the turn is computed as follows:

$$T_{st} = T_{pn+1} - \left(\frac{RMIN}{V}\right) \tan \left|\frac{\Delta\psi}{2}\right| \qquad \text{(C5)}$$

and the time in the turn is given by

$$T_T = \left|\frac{\Delta\psi}{\dot{\psi}}\right| \qquad \text{(C6)}$$

where

$RMIN = V^2/g \tan\ (20°)$

$\Delta\psi$ = heading change in turn

An error vector is computed between the reference vehicle's position and velocity and the actual aircraft's position and velocity as shown in Figure C1 and given below:

$$\bar{E} = \left[\Delta X\ \Delta Y\ \Delta Z\ \Delta\dot{X}\ \Delta\dot{Y}\ \Delta\dot{Z}\right]^T \qquad \text{(C7)}$$

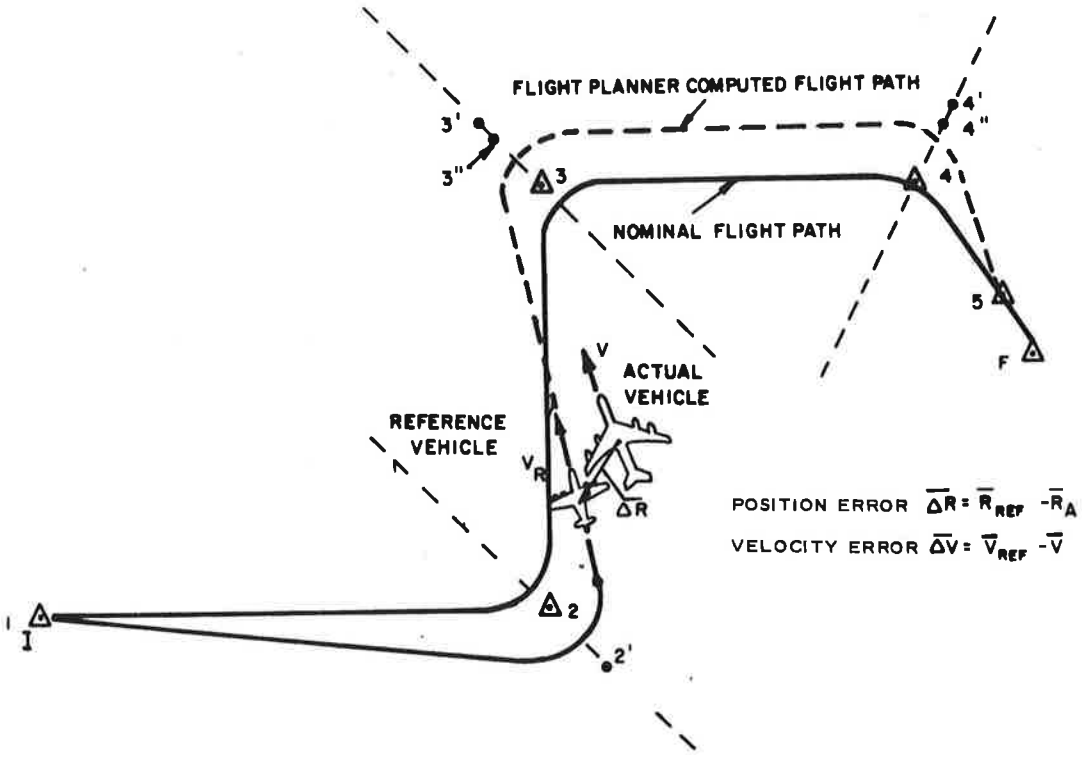

Figure C1. Error Vector from Reference Vehicle

This error vector is next transformed into the following velocity to be gained vector

$$\begin{bmatrix} V_{GX} \\ V_{GY} \\ V_{GZ} \end{bmatrix} = \begin{bmatrix} 1/T_c & 0 & 0 & 1 & 0 & 0 \\ 0 & 1/T_c & 0 & 0 & 1 & 0 \\ 0 & 0 & 1/T_z & 0 & 0 & 1 \end{bmatrix} \bar{E} \qquad \text{(C8)}$$

where T_c and T_z are characteristic times associated with the time desired to remove a position error.

The velocity to be gained vector is then transformed to an aircraft vertical heading reference frame as follows:

$$\begin{bmatrix} V_{GX} \\ V_{GY} \\ V_{GZ} \end{bmatrix}_{VH} = \begin{bmatrix} \cos \psi_A & \sin \psi_A & 0 \\ -\sin \psi_A & \cos \psi_A & 0 \\ 0 & 0 & 1 \end{bmatrix} \begin{bmatrix} V_{GX} \\ V_{GY} \\ V_{GZ} \end{bmatrix}_I \quad \text{(C9)}$$

where ψ_A is the heading of the aircraft.

The speed control and steering equations are derived from this velocity to be gained vector in the following manner:

$$\begin{bmatrix} \Delta U_c \\ \phi_c \\ \theta_c \end{bmatrix} = \begin{bmatrix} K_{11} & 0 & 0 \\ 0 & K_{22} & 0 \\ 0 & 0 & K_{33} \end{bmatrix} \cdot \begin{bmatrix} V_{GX} \\ V_{GY} \\ V_{GZ} \end{bmatrix}_{VH} \quad \text{(C10)}$$